Steering of a bosonic mode with a double quantum dot

T. Brandes and N. Lambert

Department of Physics, University of Manchester Institute of Science and Technology (UMIST), P.O. Box 88,
Manchester M60 1QD, United Kingdom
(Received 1 October 2002; published 31 March 2003)

We investigate the transport and coherence properties of a double quantum dot coupled to a single damped boson mode. The numerical results reveal how the properties of the boson distribution can be steered by altering parameters of the electronic system such as the energy difference between the dots. Quadrature amplitude variances and the Wigner function are employed to illustrate how the state of the boson mode can be controlled by a stationary electron current through the dots.

I. INTRODUCTION

The two-level system coupled to a single bosonic mode (Rabi Hamiltonian[1]) is probably one of the best-studied models for the interaction of matter with light.[2] Cavity quantum electrodynamics is an example where the coupling between atoms and photons can be studied in detail and used in order to, e.g., transfer quantum coherence from light to matter (control of tunneling by electromagnetic fields[3,4]) and vice versa.[5–7]

Quantum optics usually deals with *closed* two-level systems where the total electron number on individual atoms remains constant and does not fluctuate during the interaction with the photon. This restriction can be lifted in semiconductor quantum dots (artificial atoms) by tunnel coupling to electron reservoirs. For example, in semiconductor cavity quantum electrodynamics,[8] the interaction of light with excitons can be steered by "pumping" the cavity by resonant tunneling of electrons and holes.

In this paper, we examine a single bosonic mode interacting with a system of two (bound) electronic states which are themselves coupled to a continuum of free electrons. As a concrete realization, we investigate the stationary electron transport through a double quantum dot coupled to electron reservoirs and a single photon or phonon mode. The main idea is to control the density matrix of the coupled dot-boson system by external parameters such as the reservoir chemical potentials and the tunnel couplings. These parameters (which in experiments can be controlled via gate voltages) then determine the reduced density operators of the dot and the boson and allow one, e.g., to modify the state of the boson by driving a stationary electron current through the dots.

One of the motivations for our work are experiments in double quantum dots where the coherent coupling between classical light (microwaves) and electrons can be detected in electronic transport.[9–12] The open two-level-boson model describes the full quantum version of these systems with the light replaced by a photon field with its own quantum dynamics.

On the other hand, quantum effects (such as spontaneous emission) relevant for transport through double dots have been found to be due to *phonons* rather than photons. In fact, the importance of electron-phonon coupling for transport in coupled dots is well-established by now.[13–17] Suggestions

have been made[14,18,19] to explore "semiconductor phonon cavity QED" in nanostructures where phonons become experimentally controllable. In contrast to standard semiconductor cavity QED,[8] boundary conditions for *vibration* modes lead to extremely nonlinear phonon-dispersion relations. For example, Van Hove singularities in the phonon density of states show up at certain frequencies,[18] signatures of which seem to be relevant for transport through quantum dots embedded into free-standing structures.[20] Such a situation would then be described (within a strongly idealized model) by the coupling of a single frequency boson mode to a few-level quantum dot.

The influence of nanomechanical vibrational properties on single-electron tunneling in fact has emerged as a whole new area of mesoscopic transport, triggered by the possibility to explore electron transport through individual molecules[21–25] or in free-standing[26–29] and movable[30–33] nanostructures. Phonons then are no longer a mere source of dissipation but become experimentally controllable with the possibility, e.g., to create phonon confinement[18,34–36] or the *analogon* of quantum optical phenomena such as coherent and squeezed phonon states.[37–40]

The paper is organized as follows. In Sec. II, we introduce the model and derive a master equation for the density operator. We discuss transport properties in Sec. III where a comparison to analytical solutions is made. In Sec. IV, the reduced boson density operator, its Wigner function, and the fluctuation properties of the boson mode under a stationary electron current are discussed. Finally, we conclude with a discussion in Sec. V.

II. MODEL AND METHOD

We consider an idealized situation of a single-cavity boson mode (photon or phonon) coupled to a two-level electronic system (dot) which itself is connected to external electron reservoirs. Our aim is to determine the stationary reduced density operator $\rho(t)$ of the dot-boson system for large times t, treating the dot and the boson on equal footing. The single bosonic mode (photon or phonon) interacts with the electrons within the dots. We set $\hbar = 1$ in the following.

A. The Hamiltonian

An artificial "open" two-level system can be realized by two quantum dots (which for simplicity we call "left" and

"right") coupled to each other by a tunnel barrier and to a left source and right drain electron reservoir with chemical potentials μ_L and μ_R. In the following, we are only interested in the regime of high bias voltage $V = \mu_L - \mu_R > 0$. We assume that the charging energy U required to add an additional electron to the double dot is much greater than V (strong Coulomb blockade regime). Therefore, electrons tunnel through the structure only from the left to the right. Only one additional electron can tunnel into the double dot at a time, and the effective Hilbert space of the electronic system can be defined by three states[10,16] empty, left, and right, $|0\rangle = |N_L, N_R\rangle$, $|L\rangle = |N_L+1, N_R\rangle$, and $|R\rangle = |N_L, N_R+1\rangle$. The energies of the two states with an additional electron in the left (right) dot are denoted as ε_L (ε_R). Higher excited states for both dots are assumed to lie outside the energy window

$$\mu_L \gg \varepsilon_L, \varepsilon_R \gg \mu_R, \qquad (1)$$

which defines the regime where nonlinear transport does not significantly depend on μ_L and μ_R at low temperatures. This corresponds to the standard situation[10,14,16] where only the two lowest hybridized electronic states in the double dot contribute to transport.

The Hamiltonian H_D of the double dot is given in terms of the dot operators $n_L := |L\rangle\langle L|$, $n_R := |R\rangle\langle R|$, and a term H_T describing the tunneling between the left and the right dot,

$$H_D = H_A + H_T \equiv \varepsilon_L n_L + \varepsilon_R n_R + T_c(P + P^\dagger),$$

$$P = |L\rangle\langle R|, \quad P^\dagger = |R\rangle\langle L|. \qquad (2)$$

The tunnel matrix element T_c is used to describe the strength of the tunneling process.

The Hilbert space of the bosonic system is spanned by the usual number or Fock eigenstates $|n\rangle, n = 0,1,2,3, \ldots$ of the harmonic oscillator

$$H_p = \omega a^\dagger a \qquad (3)$$

with frequency ω and creation/annihilation operators a and $a^\dagger$ fulfilling $[a, a^\dagger] = 1$. The coupling between the electronic and the bosonic system is described by four microscopic coupling constants,

$$H_{ep} = (\alpha n_L + \beta n_R + \gamma^* P + \gamma P^\dagger)(a + a^\dagger). \qquad (4)$$

Here, we assume the coupling constants α, β, and γ as given parameters. Their precise form can be calculated from microscopic details such as the many-body wave functions of the dot electrons. It should be noted that the interaction between the bosonic system and the reservoirs is not considered here.

The two electron reservoirs are described by

$$H_{res} = \sum_k \varepsilon_k^L c_k^\dagger c_k + \sum_k \varepsilon_k^R d_k^\dagger d_k, \qquad (5)$$

where the sum is over all wave vectors k in both the left (L) and right (R) reservoirs and spin polarization is assumed for simplicity. The coupling between dot and reservoirs is described with two dot operators

$$s_L = |0\rangle\langle L|, \quad s_R = |0\rangle\langle R|; \qquad (6)$$

and the tunnel Hamiltonian

$$H_V = \sum_k (V_k^L c_k^\dagger s_L + V_k^R d_k^\dagger s_R + \text{c.c}) \qquad (7)$$

with tunnel matrix elements V_k^L and V_k^R.

The total Hamiltonian is written as

$$H = H_0 + H_T + H_V + H_{ep}, \qquad (8)$$

where $H_0 = H_A + H_p + H_{res}$ is the free Hamiltonian in the interaction picture introduced below.

B. Equations of motion

The density matrix of the total system (dot, boson, and reservoirs) is given by the Liouville–von Neumann equation and formulated in the interaction picture with respect to H_0. For the nonlinear transport window, Eq. (1) considered here, the chemical potentials in the equilibrium reservoirs are such that the Fermi distributions in the left and the right leads can well be approximated by $f_L(\varepsilon) = 1$ and $f_R(\varepsilon) = 0$. We treat the reservoir coupling term H_V in second-order perturbation theory, neglecting Kondo physics[41] throughout, so that transport can be described by a master equation.[10,16,42,43] Transforming back into the Schrödinger picture will produce the following master equation for the reduced density operator of the system (dot + boson),

$$\frac{d}{dt}\rho(t) = -i[H_A + H_p + H_T + H_{ep}, \rho(t)]$$

$$- \frac{\Gamma_L}{2}[s_L s_L^\dagger \rho(t) - 2 s_L^\dagger \rho(t) s_L + \rho(t) s_L s_L^\dagger]$$

$$- \frac{\Gamma_R}{2}[s_R^\dagger s_R \rho(t) - 2 s_R \rho(t) s_R^\dagger + \rho(t) s_R^\dagger s_R]$$

$$- \frac{\gamma_b}{2}(2 a \rho a^\dagger - a^\dagger a \rho - \rho a^\dagger a). \qquad (9)$$

The perturbation from the reservoir is given by the tunnel rates

$$\Gamma_{L/R} = 2\pi \sum_k |V_k^{L/R}|^2 \delta(\varepsilon_{L/R} - \varepsilon_k^{L/R}). \qquad (10)$$

In the last line in Eq. (9), we introduced a term that describes damping of the bosonic system at a rate γ_b (Ref. 44) corresponding to photon or phonon cavity losses.

Taking matrix elements of the master equation, Eq. (9), one obtains a system of linear equations for the matrix elements of the density operator which are given explicitly in Appendix A. In the stationary state of these equations, the time derivatives are zero, and a coupled set of linear equations is found. In order to numerically solve these equations, the bosonic Hilbert space has to be truncated at a finite number N of boson states. The total number of equations then is $5N^2 + 10N + 5$, remembering that there is always an equation for $n = m = 0$. The numerical solution becomes a standard matrix inversion, though book-keeping of the matrix

elements has to be done carefully. The trace over electron and boson degrees of freedom has to obey the normalization condition

$$\sum_n \left[\langle n,0|\rho_{stat}|n,0\rangle + \langle n,R|\rho_{stat}|n,R\rangle + \langle n,L|\rho_{stat}|n,L\rangle \right] = 1. \quad (11)$$

We mention that without this condition, the matrix becomes singular, and cannot be solved.

III. TRANSPORT PROPERTIES

The first quantity of interest that one can obtain from the matrix elements is the stationary electron current through the double dot.

A. Stationary current: numerical results

In the stationary state, the current operator is defined via the rate of electrons tunneling from the left dot to the right dot,

$$\hat{I} = \frac{\partial}{\partial t} n_L = iT_C(P^\dagger - P) + i(\gamma P^\dagger - \gamma^* P)(a + a^\dagger). \quad (12)$$

Here and in the following, we set the electron charge $-e = 1$. For a boson mode with wave vector $\mathbf{Q}$, the electron-boson coupling constants can be expressed in terms of matrix elements of the left and right dot states, $\alpha = \lambda\langle L|e^{i\mathbf{Qr}}|L\rangle$, $\beta = \lambda\langle R|e^{i\mathbf{Qr}}|R\rangle$, $\gamma = \lambda\langle L|e^{i\mathbf{Qr}}|R\rangle$, where λ is the microscopic constant for the interaction of the boson with the electron in two dimensions.

Our formalism works for arbitrary choices of coupling parameters α, β, γ, but for simplicity we restrict ourselves to simple, nontrivial cases for the numerical calculations. We set $\gamma = 0$, which corresponds to neglecting the nondiagonal terms which for relatively sharp peaked electron densities in the dots only weakly contribute.[45] For a sharp electron density profile, one further has $\beta = \alpha e^{i\mathbf{Qd}}$, where $\mathbf{d}$ is the vector connecting the left and right dot centers. Identical energy shifts in both dots, corresponding to $\beta = \alpha$, have no effect on transport. In the following, we choose $\mathbf{Qd} = \pi$ and therefore electron-boson coupling constants are

$$\alpha = -\beta \equiv 2g, \quad \gamma = 0. \quad (13)$$

Furthermore, the tunneling rates between the reservoirs and the dots are generally kept smaller than the energies of the dots and boson states. This produces clear and sharply defined transport characteristics. We use the boson frequency as an energy scale and set $\omega = 1$ in the following. Using the typical phonon cavity energy $\hbar\omega \approx 100~\mu$eV from a recent experiment with a free-standing phonon cavity[20] will yield a typical electron current scale of $e\omega = 24$ nA, as shown in Figs. 1 and 2.

Figure 1 illustrates the stationary current as a function of the energy difference ε. For zero boson coupling $g = 0$, we reproduce the Lorentzian resonant tunneling profile

$$I_{stat} = T_c^2 \Gamma_R / [T_c^2(2 + \Gamma_R/\Gamma_L) + \Gamma_R^2/4 + \varepsilon^2] \quad (14)$$
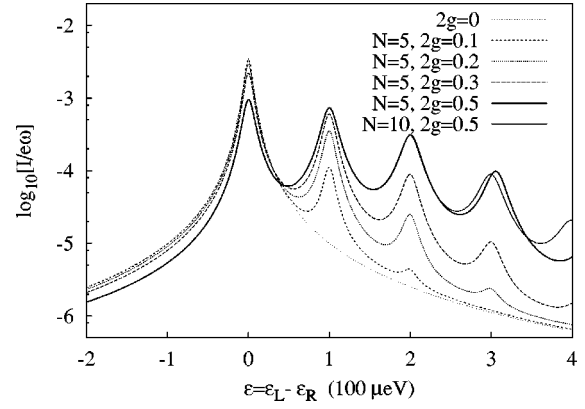

FIG. 1. Stationary current through double quantum dot coupled to single boson mode with $\Gamma_L = \Gamma_R = 0.1$, $T_c = 0.01$, $\gamma_b = 0.05$, and varying $2g = \alpha = -\beta$. [Electron-boson coupling, cf. Eq. (4)]. N: number of boson states.

as first derived by Stoof and Nazarov.[10]

For finite electron-boson coupling and positive ε, resonances appear when

$$\varepsilon \equiv \varepsilon_L - \varepsilon_R = n\omega, \quad (15)$$

i.e., the energy gap of the dots becomes equal to multiple integers of the boson energy. At these resonances, electrons tunneling from the left to the right dot can excite the boson system.

The current profiles with differing damping rates, Fig. 2, illustrate that the system is extremely sensitive even to very small "damping." For small but finite boson damping, we found that two profiles for $N = 5$ and $N = 10$ match in an extremely close manner. This illustrates that a finite boson damping removes numerical problems due to the truncation of the boson Hilbert space at a finite N. As expected, there are no peaks at all on the absorption side of the profile ($\varepsilon < 0$): the damped boson relaxes to its ground state.
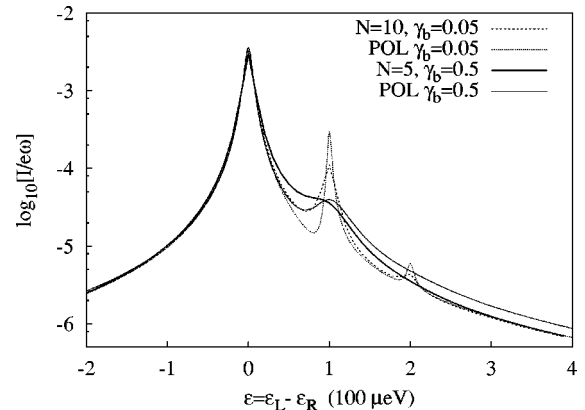

FIG. 2. Current as in Fig. 1 for coupling $2g = 0.1$ and different boson damping γ_b, alongside corresponding polaron transformation result, Eq. (19).

B. Perturbation theory in T_c: Polaron transformation method

An analytical expression for the stationary current can be obtained from a polaron transformation and a polaron-transformed master equation that is valid for small coupling T_c between the two dots.[16] After tracing out the bosonic degrees of freedom, one obtains an equation of motion for the time-dependent expectation values of the operators $n_{L/R}$ and $P^{(\dagger)}$ which can be transformed into the Laplace space,

$$\langle n_L \rangle(z) = -i\frac{T_c}{z}\{\langle P \rangle(z) - \langle P^\dagger \rangle(z)\} + \frac{\Gamma_L}{z}\{1/z - \langle n_L \rangle(z)$$

$$- \langle n_R \rangle(z)\},$$

$$\langle n_R \rangle(z) = i\frac{T_c}{z}\{\langle P \rangle(z) - \langle P^\dagger \rangle(z)\} - \frac{\Gamma_R}{z}\langle n_R \rangle(z),$$

$$\langle P \rangle(z) = -iT_c\{\langle n_L \rangle(z)C_\varepsilon(z) - \langle n_R \rangle(z)C^*_{-\varepsilon}(z)\}$$

$$- \frac{\Gamma_R}{2}\langle P \rangle(z)C_\varepsilon(z). \tag{16}$$

Here, the coupling to the boson system enters through the correlation function

$$C_\varepsilon(z) = \int_0^\infty dt\, e^{-zt + i\varepsilon t} C(t),$$

$$C(t) = \langle X(t)X^\dagger(t=0) \rangle, \quad X = D\left(\frac{4g}{\omega}\right) \tag{17}$$

of the displacement operator of the bosonic mode,

$$D(\xi) = \exp(\xi a^\dagger - \xi^* a). \tag{18}$$

Equations (16) can be solved algebraically. One then obtains the expectation value $\langle I \rangle_{t\to\infty}$ of the stationary current from the $1/z$ coefficient of the $I(z)$ expansion into a Laurent series[46] for $z\to 0$,

$$\langle I \rangle_{t\to\infty} = T_c^2 \frac{2\mathrm{Re}(C_\varepsilon) + \Gamma_R|C_\varepsilon|^2}{\left|1 + \frac{\Gamma_R}{2}C_\varepsilon\right|^2 + 2T_c^2 B_\varepsilon},$$

$$B_\varepsilon := \mathrm{Re}\left\{\left(1 + \frac{\Gamma_R}{2}C_\varepsilon\right)\left[\frac{C_{-\varepsilon}}{\Gamma_R} + \frac{C^*_\varepsilon}{\Gamma_L}\left(1 + \frac{\Gamma_L}{\Gamma_R}\right)\right]\right\}, \tag{19}$$

where $C_\varepsilon \equiv C_\varepsilon(z\to 0)$.

The correlation function $C(t)$ enters via a factorization assumption in the polaron-transformed master equation and has to be calculated from an effective density operator ρ_B of the bosonic mode. For dissipative pseudospin-boson systems with a continuous spectrum of modes and a thermal equilibrium for ρ_B, reasonable results can be obtained within this method for small coupling, in particular, in comparison with perturbation theory.[45,47] However, in the present case with just one single mode it is not clear whether or not a factorization into an effective dot and an effective boson density operator yields reasonable results, and in principle, one

should at least determine ρ_B self-consistently. For small couplings g, however, the assumption of a decoupled time evolution of the boson should work well, and we proceed with a master equation for ρ_B,

$$\frac{d}{dt}\rho_\mathrm{B}(t) = -i[\omega a^\dagger a, \rho_\mathrm{B}] - \frac{\gamma_b}{2}(2a\rho_\mathrm{B}a^\dagger - a^\dagger a\rho_\mathrm{B} - \rho_\mathrm{B}a^\dagger a) \tag{20}$$

that describes the free time evolution of the boson in presence of boson damping with damping constant $\gamma_b > 0$. Assuming the boson initial condition to be its ground state, one obtains ($t > 0$)

$$C(t) = \exp\{-|\xi|^2(1 - e^{-[(\gamma_b/2) + i\omega]t})\}, \quad \xi = \frac{4g}{\omega}. \tag{21}$$

Figure 2 shows that the analytical expression for the current, Eq. (19), compares quite well with the numerical results. In particular, this demonstrates that the formulation in terms of a general boson correlation function $C(t)$ works reasonably well not only for boson systems with continous mode spectrum,[16,45] but also for the single mode case discussed here, at least for small-coupling constants g. We point out that the existence of a finite boson damping is crucial here and that for larger g, the comparison becomes worse, as expected.

IV. BOSON DISTRIBUTION

Turning now to properties of the bosonic system, our primary interest is in how the boson mode can be controlled via parameters of the electron subsystem such as the bias ε and the tunnel couplings $\Gamma_{R/L}$. In the stationary state, the reduced density operator of the boson is

$$\rho_b \equiv \lim_{t\to\infty}\mathrm{Tr}_\mathrm{dot}\rho(t) = \lim_{t\to\infty}\sum_{i=0,L,R}\rho^{ii}(t). \tag{22}$$

A. Boson state detection

Before discussing the boson state ρ_b, we describe a possible experimental scheme to directly detect its properties. The basic idea is to use another nearby double quantum dot as detector of the boson, similar to the scheme for detecting quantum noise in mesoscopic conductors as proposed by Aguado and Kouwenhoven.[48]

The detector consists of a double quantum dot very similar to the one discussed above. The boson state gives a contribution to the inelastic, stationary current

$$I_d(E) \approx T_d^2 P(E) = 2T_d^2 \mathrm{Re}\int_0^\infty dt\, e^{iEt}C_d(t);$$

$$C_d(t) = \mathrm{Tr}[\rho_b X_d(t)X_d^\dagger], \quad X_d = D\left(\frac{4g_d}{\omega}\right) \tag{23}$$

through the detector in the lowest order in the detector tunnel coupling T_d. Here, E denotes the detector dot energy difference, D again denotes the unitary displacement operator, Eq.

(18), g_d the coupling constant in the detector double dot, and ρ_b the boson state. Equation (23) describes the detector current $I(E)$ resulting from a given boson state ρ_b, as calculated in the following section.

Before discussing our numerical results for ρ_b, it is illustrative to look at a few special cases. For example, if the boson state ρ_b describes a thermal equilibrium at temperature T, one obtains the inelastic current spectrum with absorption $E<0$ and emission $E>0$ branches[16], as has been observed by Fujisawa *et al.*[14] for the case of equilibrium (multimode) phonons.

If $\rho_b=|n\rangle\langle n|$ describes a pure, n-boson number state, the function $C_d(t)$ in the detector current, Eq. (23), becomes ($\xi=4g_d/\omega$)

$$C_d(t)=\langle n|D(\xi e^{i\omega t})D(-\xi)|n\rangle$$
$$=e^{-i|\xi|^2\sin\omega t}e^{-(1/2)|\xi(1-e^{i\omega t})|^2}L_n^0(|\xi(1-e^{i\omega t})|^2),$$
(24)

where L_n^0 is a Laguerre polynomial, cf. Appendix B. Here we assume that the boson time evolution is undamped in the detector, i.e., governed by the boson Hamiltonian $H_b=\omega a^\dagger a$. Expanding up to the lowest order in $\xi=4g_d/\omega$ and using $L_n^0(x)=1-nx+O(x^2)$, one obtains from Eqs. (23) and (24),

$$I_d(E)\approx T_d^2 2\pi[\{1-|\xi|^2(2n+1)\}\delta(E)+|\xi|^2\{n\,\delta(E+\omega)$$
$$+(n+1)\delta(E-\omega)\}].$$
(25)

Clearly, the height of the inelastic current peaks is determined by the quantum number n, i.e., the absorption peak at $E=-\omega<0$ scales with n, and the (stimulated) emission peak at $E=\omega>0$ scales with $n+1$.

The above example can be even generalized. In Appendix C we show how to reconstruct an arbitrary boson state $\rho_b=\Sigma_{nm}\rho_{nm}|n\rangle\langle m|$ from the function $P(E)$ [or equivalently the stationary detector current spectrum $I_d(E)$, Eq. (23)]. This demonstrates that the properties of the boson state discussed in the following can be directly related to an experimentally accessible quantity.

B. Numerical results

We first analyze the boson mode via moments of its distribution function such as occupation number and Fano factor before discussing the full distribution function in the Wigner function representation.

The boson occupation probability $p_n=(\rho_b)_{nn}$ is the probability for the boson to be in one particular number state n. Furthermore, the boson Fano factor F^Q is calculated from the boson occupancy as the variance of boson number over the mean number of bosons,

$$F^Q=\frac{\langle\hat{n}^2\rangle-\langle\hat{n}\rangle^2}{\langle\hat{n}\rangle}.$$
(26)

Similarly, the variance $\Delta x^2=\langle x^2\rangle-\langle x\rangle^2$ and $\Delta p^2=\langle p^2\rangle-\langle p\rangle^2$ of the position and a momentum coordinate
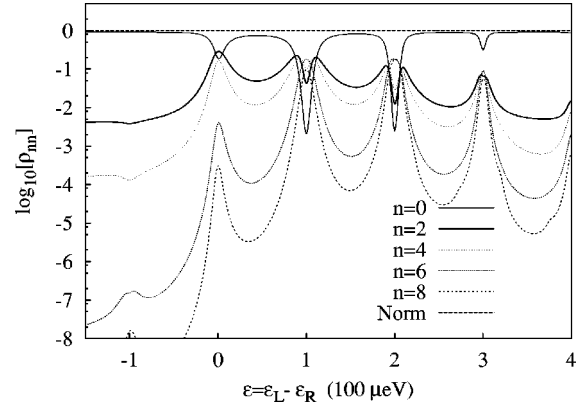

FIG. 3. Boson profiles $n=0,2,4,\dots,10$ for $\gamma_b=0.0001$, $N=10$, $2g=\alpha=-\beta=0.3$, $10T_C=\Gamma_L=\Gamma_R=0.1$.

$$x=\frac{(a+a^\dagger)}{\sqrt{2}}, \quad p=\frac{i(-a+a^\dagger)}{\sqrt{2}}$$
(27)

can be obtained from ρ_b, cf. Eq. (A7) in Appendix A. They provide an indication of the quantum fluctuations in the boson states, and prove useful in comparison with the Fano factor profile. It should also be apparent that $\Delta x^2\Delta p^2\geq\frac{1}{4}$.

We have checked that the probability p_n fulfills the normalization $\Sigma_n p_n=1$. For accurate results, the occupation probability should tend to 0 as $n\rightarrow N$, where N is the dimension of the truncated boson Hilbert space. This condition is easily achieved in presence of a finite boson damping rate, $\gamma_b>0$. In this case, it is possible to obtain a boson distribution which is centered around the lower boson number states, and is excited when a resonant interaction with the electron occurs.

It is more illustrative to first discuss a weakly damped case, as shown in Fig. 3. We can see quite clearly how at the positive resonance energies, the occupation probabilities of the states spread into the higher number states.

The Fano factor F^Q illustrates fluctuation properties of the boson mode with $F^Q=1$ corresponding to a Poissonian boson number distribution and $F^Q<1$ ($F^Q>1$) to a sub (super)-Poissonian distribution. Figure 4 illustrates the Fano factor vs ε for the strongly damped case.

This profile suggests the reduced boson states are coherent (Poissonian) for $\varepsilon<0$, and super-Poissonian at the resonance energies, $\varepsilon=\omega,2\omega,\dots$.

C. Coherent state and x-p variances

For $\varepsilon\ll0$, nearly no current is flowing, the electron is predominantly localized in the left dot, and one can approximate the operator $\sigma_z=|L\rangle\langle L|-|R\rangle\langle R|$ by its expectation value $\langle\sigma_z\rangle=1$. Then, the boson system is effectively described by

$$H_{\text{eff}}=2g(a+a^\dagger)+\omega a^\dagger a,$$
(28)

which is a shifted oscillator, the ground state $|GS\rangle$ of which is the coherent state $|GS\rangle=|-2g/\omega\rangle$ with $a|z\rangle=z|z\rangle$. This
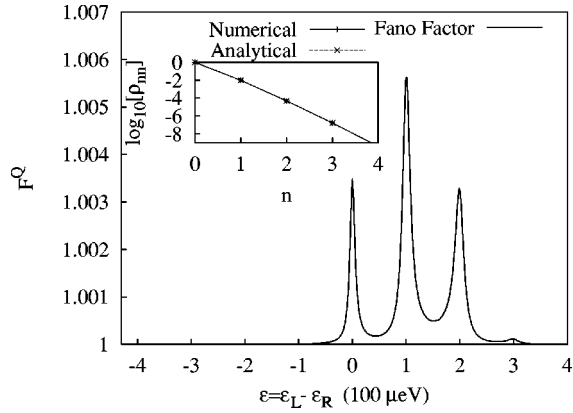
FIG. 4. Fano vs ε profile for $2g=\alpha=-\beta=0.1$, $N=10$, $\gamma_b=0.05$, $10T_C=\Gamma_L=\Gamma_R=0.1$. Inset: Comparison between coherent state, Eq. (29), and numerical result for boson distribution p_n at $\varepsilon=-4$.

can be seen by introducing new operators $b:=a+2g/\omega$ whence $H_{eff}=\omega b^\dagger b-4g^2/\omega$ and $b|GS\rangle=0$. In this regime, we have

$$\rho_b\approx|z\rangle\langle z|, \quad z=-2g/\omega, \qquad (29)$$

and $p_n=|\langle n|GS\rangle|^2$ is given by a Poisson distribution, $p_n=|z|^{2n}e^{-|z|^2}/n!$. One can plot this against the numerically obtained p_n and check that the distribution is indeed Poissonian for small $\varepsilon\ll 0$. This is represented in the inset of Fig. 4 in detail for the first four-boson Fock (number) states.

The quantum fluctuations of the boson system are described by the variance of the position and momentum operators. Figure 5 presents a direct comparison of the position and momentum variance of a strongly damped system. The uncertainty principle holds, $\Delta x\Delta p\geq\frac{1}{2}$, and thus $\Delta x^2\Delta p^2\geq\frac{1}{4}$. The state with minimum uncertainty occurs as expected, for $\varepsilon_L<\varepsilon_R$, with $\Delta x^2\Delta p^2=\frac{1}{4}$. This is a reassuring result, since it suggests both that the boson is coherent in this area, and that the Fano factor's Poissonian distribution for this coherent state is correct. We mention that since both $\Delta x>0.5$ and $\Delta p>0.5$, we find no squeezing of the boson mode for the parameters checked here.
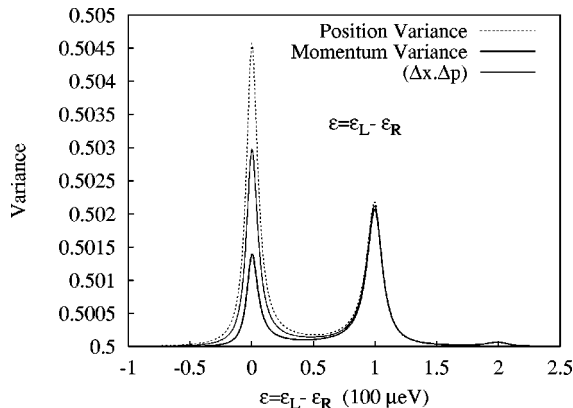
FIG. 5. Position variance, momentum variance, and an estimation of the combined uncertainty. $2g=\alpha=-\beta=0.1$, $N=10$, $\gamma_b=0.05$, $10T_C=\Gamma_L=\Gamma_R=0.1$.

D. Wigner function

The Wigner function of the density operator ρ_b for a bosonic mode $a^\dagger$ is a representation of ρ_b in x-p space, cf. Eq. (27). It is defined as[49]

$$W(x,p):=\frac{1}{\pi}\text{Tr}(\rho_b D(2\alpha)U_0), \quad \alpha=\frac{x+ip}{\sqrt{2}}, \qquad (30)$$

where $D(\alpha):=\exp[\alpha a^\dagger-\alpha^* a]$, Eq. (18), is a unitary displacement operator and $U_0:=\exp[i\pi a^\dagger a]$ is a parity operator for the boson.[50] $W(x,p)$ is a symmetric Gaussian for a pure coherent boson state and a symmetric Gaussian multiplied with a polynomial for a pure number state.[44] In our model, the shape of $W(x,p)$ therefore indicates how close to these limiting cases the actual stationary state ρ_b of the boson, Eq. (22), is. In particular, this is a convenient way to represent the "steering" of the boson mode when external parameters (such as ε or $\Gamma_{R/L}$) are changed.[51]

Using the Fock state basis $\{|n\rangle, n=0,1,2,\dots\}$ and $U_0=\Sigma_{n=0}^\infty(-1)^n|n\rangle\langle n|$, we find

$$W(x,p)=\frac{1}{\pi}\sum_{n,m=0}^\infty(-1)^n\langle n|\rho_b|m\rangle\langle m|D(2\alpha)|n\rangle. \qquad (31)$$

It is useful to split the sum into diagonal and nondiagonal parts, to use $\langle m|\rho_b|n\rangle=\langle n|\rho_b|m\rangle^*$; and $(m\geq n)$

$$\langle m|D(\alpha)|n\rangle=\sqrt{\frac{n!}{m!}}\alpha^{m-n}e^{-(1/2)|\alpha|^2}L_n^{m-n}(|\alpha|^2)$$

$$=\langle m|D^\dagger(\alpha)|n\rangle^*=(-1)^{m-n}\langle m|D(\alpha)|n\rangle^*, \qquad (32)$$

where again $\alpha=(x+ip)/\sqrt{2}$ and L_n^{m-n} is a Laguerre polynomial, cf. Appendix B. This leads to

$$W(x,p)=\frac{1}{\pi}\sum_{n=0}^\infty(-1)^n\langle n|\rho_b|n\rangle\langle n|D(2\alpha)|n\rangle$$

$$+\frac{1}{\pi}\sum_{n=0}^\infty\sum_{m=n+1}^\infty(-1)^n 2\,\text{Re}[\langle n|\rho_b|m\rangle$$

$$\times\langle m|D(2\alpha)|n\rangle]. \qquad (33)$$

Using our numerical results for the stationary state ρ of the coupled system, we easily obtain Wigner functions from Eqs. (22) and (33) for different values of the energy difference ε between the two dots as shown in Fig. 6. Between two resonance energies $\varepsilon=n\omega$, $W(x,p)$ closely resembles a Gaussian. At and close to the resonance energies, the distribution spreads out in rings around the origin, which is consistent with the increased Fock state occupation numbers and the increased position and momentum variances at these energies.
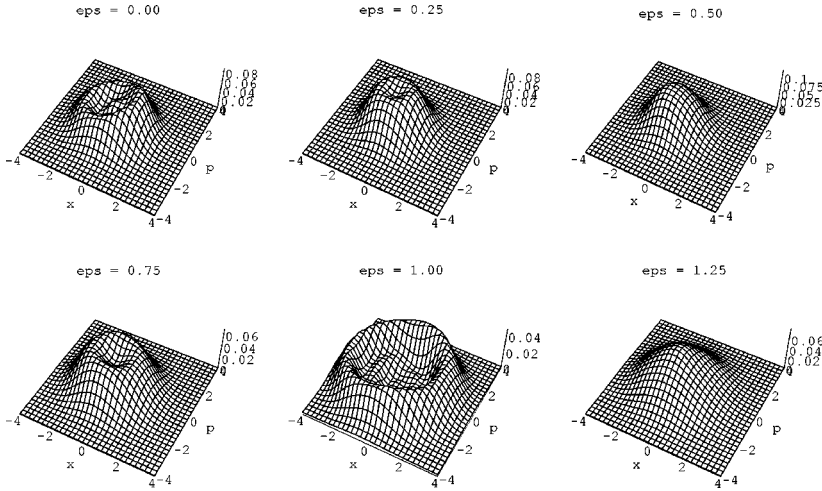
FIG. 6. Wigner distribution functions for the bosonic mode. Parameters are $\Gamma_L = \Gamma_R = T_c = 0.1$, $\gamma_b = 0.005$, $g = 0.2$, $N = 20$. Stationary current resonances occur at $\varepsilon = 0.0, 1.0, 2.0, \ldots$.

V. DISCUSSION

Our investigation is based on a numerical method which allows the density matrix of the boson-dot system to be solved for arbitrary dot parameters (ε, T_c, $\Gamma_{L/R}$) and boson damping rate γ_b. Since we have to truncate the boson Hilbert space, the electron-boson coupling constant g has to be restricted to small values $g \lesssim 1$. In contrast with the determination of the (pure) eigenstates of an isolated dot-boson system (Rabi Hamiltonian), the numerical effort for our mixed state (density operator) is much bigger here. Although not discussed in this paper, we suggest that the strong-coupling regime could be reached numerically by a polaron transformation of the master equation[16] without the factorization assumption employed in Sec. III B. Fortunately, at present the small-coupling regime seems to be valid for experimental situations with quantum dots.[13–16]

Our results suggest that there is no resonant interaction on the $\varepsilon < 0$ side of the current peak as long as the boson system is damped and any many-body excited electron states can be ignored. For $\varepsilon > 0$, we have found strong excitations of the boson mode occurring at resonances given by multiples $n\omega$ of the boson frequency ω. These correspond to the photo-satellite peaks in resonant tunneling in electromagnetic ac fields[9,10] which in the classical case, however, appear on both sides of the main resonance $n = 0$ in contrast with the quantum case considered here. The resonances at $\varepsilon = n\omega$ can thus be interpreted as the emission of phonons (photons) by the electron as it tunnels through the dot. It should be possible to detect them in the stationary current through double quantum dots in phonon resonators. With increasing electron-boson coupling, the visibility of these side peaks increases whereas the main resonance at $\varepsilon = 0$ is reduced.

We have discussed that an additional double dot can serve as a detector of the stationary boson state ρ_b, if its energy difference E is tuned independently. In the single mode case considered here, the stationary detector current spectrum $I_d(E)$ is uniquely related to the components of ρ_b in the number state basis. In order to characterize the stationary boson state itself, we have investigated the Fano factor and the quantum fluctuations in the quadrature amplitudes of the boson. For $\varepsilon \ll 0$, the boson state is perfectly described as a coherent state whereas for $\varepsilon \gtrsim 0$, the interaction with the quantum dot produces occupied excited states in the boson mode that could best be visualized by a broadening of the phase-space (Wigner) distribution function of the boson.

Although in this paper we have only calculated stationary properties, our method can be extended to calculate the noise spectrum via the quantum regression theorem within the master-equation framework as well.[44] It remains a task for the future to analyze the relation between the boson quantum fluctuations and the current noise in detail.

APPENDIX A: MATRIX ELEMENTS OF THE DENSITY OPERATOR

The matrix elements of the dot-boson density operator ρ are defined as

$$\rho^i_{nm} := \langle n, i | \rho | i, m \rangle, \quad i = 0, L, R;$$

$$\rho^{ij}_{nm} := \langle n, i | \rho | j, m \rangle, \quad i, j = 0, L, R, \tag{A1}$$

where n and m refer to boson Fock states.

The matrix elements for the empty dot state obey

$$\frac{d}{dt} \rho^0_{nm} = [i\omega(m-n)\rho^0_{nm}] - \Gamma_L[\rho^0_{nm}] + \Gamma_R[\rho^R_{nm}]$$

$$+ \frac{\gamma_b}{2}[2\rho^0_{n+1,m+1}\sqrt{n+1}\sqrt{m+1} - \rho^0_{nm}(n+m)],$$

$$\tag{A2}$$

those for the right dot state

$$\frac{d}{dt}\rho_{nm}^R = i[\,\omega(m-n)\rho_{nm}^R + T_c(\rho_{nm}^{RL}-\rho_{nm}^{LR}) + \beta(\sqrt{m}\rho_{nm-1}^R$$

$$+ \sqrt{m+1}\rho_{nm+1}^R - \sqrt{n}\rho_{n-1m}^R - \sqrt{n+1}\rho_{n+1m}^R)$$

$$+ \gamma^*(\sqrt{m}\rho_{nm-1}^{RL} + \sqrt{m+1}\rho_{nm+1}^{RL}) - \gamma(\sqrt{n}\rho_{n-1m}^{LR}$$

$$+ \sqrt{n+1}\rho_{n+1m}^{LR})] - \Gamma_R[\rho_{nm}^R]$$

$$+ \frac{\gamma_b}{2}[2\rho_{n+1,m+1}^R\sqrt{n+1}\sqrt{m+1} - \rho_{nm}^R(n+m)],$$

$$(A3)$$

and for the left dot state

$$\frac{d}{dt}\rho_{nm}^L = i[\,\omega(m-n)\rho_{nm}^L + T_c(-\rho_{nm}^{RL}+\rho_{nm}^{LR})$$

$$+ \alpha(-\sqrt{n+1}\rho_{n+1m}^L - \sqrt{n}\rho_{n-1m}^L + \sqrt{m}\rho_{nm-1}^L$$

$$+ \sqrt{m+1}\rho_{nm+1}^L) + \gamma^*(-\sqrt{n+1}\rho_{n+1m}^R - \sqrt{n}\rho_{n-1m}^{RL})$$

$$+ \gamma(\sqrt{m}\rho_{nm-1}^{LR} + \sqrt{m+1}\rho_{nm+1}^{LR})] + \Gamma_L[\rho_{nm}^0]$$

$$+ \frac{\gamma_b}{2}[2\rho_{n+1,m+1}^L\sqrt{n+1}\sqrt{m+1} - \rho_{nm}^L(n+m)].$$

$$(A4)$$

The equation of motion for the off-diagonal elements ρ_{nm}^{RL} is

$$\frac{d}{dt}\rho_{nm}^{RL} = i[\,\rho_{nm}^{RL}[\omega(m-n)+(\varepsilon_L-\varepsilon_R)] + \beta(-\sqrt{n+1}\rho_{n+1m}^{RL}$$

$$- \sqrt{n}\rho_{n-1m}^{RL}) + \alpha(\sqrt{m+1}\rho_{nm+1}^{RL} + \sqrt{m}\rho_{nm-1}^{RL})$$

$$+ \gamma(-\sqrt{n+1}\rho_{n+1m}^{LL} - \sqrt{n}\rho_{n-1m}^{LL} + \sqrt{m+1}\rho_{nm+1}^{RR}$$

$$+ \sqrt{m}\rho_{nm-1}^{RR}) + T_c(\rho_{nm}^{RR}-\rho_{nm}^{LL})] - \frac{\Gamma_R}{2}[\rho_{nm}^{RL}]$$

$$+ \frac{\gamma_b}{2}[2\rho_{n+1,m+1}^{RL}\sqrt{n+1}\sqrt{m+1} - \rho_{nm}^{RL}(n+m)].$$

$$(A5)$$

Taking the trace over all the boson and electron states, Eq. (12) for the electron current operator reads

$$\langle\hat{I}\rangle = \sum_n iT_C[\rho_{n,n}^{LR}-\rho_{n,n}^{RL}] + \sum_n i[\,\gamma(\rho_{n,n-1}^{LR}\sqrt{n}$$

$$+ \rho_{n,n+1}^{LR}\sqrt{n+1}) - \gamma^*(\rho_{n,n-1}^{RL}\sqrt{n} + \rho_{n,n+1}^{RL}\sqrt{n+1})].$$

$$(A6)$$

The variances of the boson position and momentum coordinate, Eq. (27), are obtained by performing the trace over the dot variables $0,L,R,$

$$\Delta x^2 = \frac{1}{2}\text{Tr}_{\text{dot}}\sum_n [\sqrt{n}\sqrt{n-1}\rho_{n,n-2} + (2n+1)\rho_{n,n}$$

$$+ \sqrt{n+1}\sqrt{n+2}\rho_{n,n+2}] - \frac{1}{2}\left[\text{Tr}_{\text{dot}}\sum_n (\sqrt{n}\rho_{n,n-1}$$

$$+ \sqrt{n+1}\rho_{n,n+1})\right]^2,$$

$$(A7)$$

$$\Delta p^2 = \frac{1}{2}\text{Tr}_{\text{dot}}\sum_n [-\sqrt{n}\sqrt{n-1}\rho_{n,n-2} + (2n+1)\rho_{n,n}$$

$$- \sqrt{n+1}\sqrt{n+2}\rho_{n,n+2}] - \frac{1}{2}\left[\text{Tr}_{\text{dot}}\sum_n (-i\sqrt{n}\rho_{n,n-1}$$

$$+ i\sqrt{n+1}\rho_{n,n+1})\right]^2.$$

$$(A8)$$

APPENDIX B: DISPLACEMENT OPERATOR, COHERENT STATES

Here, we summarize some useful properties of the unitary displacement operator

$$D(z) \equiv e^{za^\dagger - z^*a} = (D^\dagger(z))^{-1} = D^\dagger(-z)$$

$$= e^{-(1/2)|z|^2}e^{za^\dagger}e^{-z^*a} = e^{(1/2)|z|^2}e^{-z^*a}e^{za^\dagger}, \quad (B1)$$

where z is a complex number and we used the operator exponential $e^{A+B} = e^A e^B e^{-(1/2)[A,B]}$ for $[[A,B],A] = [[A,B],B] = 0$, cf. also Ref. 44. A coherent boson state $|z\rangle$ is defined as an eigenstate of the annihilation operator, $a|z\rangle = z|z\rangle$, where z is a complex number. It can be generated from the boson vacuum $|0\rangle$ as

$$|z\rangle = D(z)|0\rangle. \quad (B2)$$

Extremely useful is the relation

$$D(\alpha+\beta) = D(\alpha)D(\beta)e^{-i\,\text{Im}(\alpha\beta^*)} \quad (B3)$$

for arbitrary complex numbers α, β. Coherent-state matrix elements of $D(\alpha)$ follow as

$$\langle\beta|D(\alpha)|\beta\rangle = e^{-(1/2)|\alpha|^2}e^{2i\,\text{Im}(\alpha\beta^*)}. \quad (B4)$$

Number state matrix elements can be obtained using $|n\rangle \equiv (1/\sqrt{n!})(a^\dagger)^n|0\rangle$,

$$\langle m|D(\alpha)|n\rangle = e^{(1/2)|\alpha|^2}\frac{1}{\sqrt{n!m!}}\frac{\partial^{n+m}}{\partial z_1^m \partial z_2^n}$$

$$\times\langle 0|e^{(z_1-\alpha^*)a}e^{(z_2+\alpha)a^\dagger}|0\rangle|_{z_1=z_2=0}.$$

$$(B5)$$

With $\langle 0|e^{(z_1-\alpha^*)a}e^{(z_2+\alpha)a^\dagger}|0\rangle = e^{(z_1-\alpha^*)(z_2+\alpha)}$ for $m \geqslant n$ the differentiation yields

$$\langle m|D(\alpha)|n\rangle = e^{(1/2)|\alpha|^2} \frac{1}{\sqrt{n!m!}} \frac{\partial^n}{\partial z_2^n}(z_2$$

$$+ \alpha)^m e^{-(z_2+\alpha)\alpha^*}\big|_{z_2=0}. \qquad \text{(B6)}$$

Comparison with the generating function of the Laguerre polynomials[51] yields Eq. (32). A corresponding expression can be derived for $n \geq m$.

APPENDIX C: RELATION BETWEEN $P(E)$ AND STATIONARY BOSON STATE ρ_b

Again we assume that the boson time evolution is undamped in the detector, i.e., governed by the boson Hamiltonian $H_b = \omega a^\dagger a$. Expressing an arbitrary boson state ρ_b in the number state basis, $\rho_b = \Sigma_{nm}\rho_{nm}|n\rangle\langle m|$, and Fourier transforming the function $P(E)$, Eq. (23), yields ($\xi = 4g_d/\omega$)

$$\tilde{P}(t) \equiv \frac{1}{2\pi}\int_{-\infty}^{\infty} dE\, e^{-iEt} P(E) = C_d(t) + C_d^*(-t)$$

$$= \sum_{nm} \rho_{nm} c_{nm}(t),$$

$$c_{nm}(t) \equiv \langle m|D(\xi e^{i\omega t})D(-\xi)|n\rangle$$

$$+ \langle m|D(\xi)D(-\xi e^{-i\omega t})|n\rangle. \qquad \text{(C1)}$$

The functions $c_{nm}(t)$ can be calculated analytically using Eq. (B4) and the matrix elements $\langle m|D(z)|n\rangle$ of the unitary displacement operator, Eq. (32). They are periodic in $2\pi/\omega$, and from integrating Eq. (C1) over one period, one obtains a linear relation between the Fourier coefficients $\tilde{P}^k$ and c_{nm}^k,

$$\tilde{P}^k = \sum_{nm} c_{nm}^k \rho_{nm},$$

$$\tilde{P}^k \equiv \frac{\omega}{2\pi}\int_0^{2\pi/\omega} \tilde{P}(t) e^{ik\omega t} dt,$$

$$c_{nm}^k \equiv \frac{\omega}{2\pi}\int_0^{2\pi/\omega} c_{nm}(t) e^{ik\omega t} dt. \qquad \text{(C2)}$$

The $\tilde{P}^k$ have to be determined by numerical integration from the (experimentally given) $P(E)$. Regarding (nm) as a single index, Eq. (C2) is a linear equation that can then be solved for the coefficients ρ_{nm} of the boson state by inverting the matrix c_{nm}^k, the coefficients of which are given as Fourier coefficients of known expressions. In practical terms, the number of boson states as well as the number of Fourier coefficients have to be restricted in order to make this inversion feasible.

Equation (C2) establishes the relation between $P(E)$ [or, via Eq. (23), the detector current $I_d = T_d^2 P(E)$ in lowest order T_d] and an arbitrary single mode boson state ρ_b.

[1] I.I. Rabi, Phys. Rev. **51**, 652 (1937).

[2] L. Allen and J.H. Eberly, *Optical Resonance and Two-Level Atoms* (Dover, New York, 1987).

[3] P. Neu and R.J. Silbey, Phys. Rev. A **54**, 5323 (1996).

[4] M. Grifoni and P. Hänggi, Phys. Rep. **304**, 229 (1998).

[5] M. Ueda, T. Wakabayashi, and M. Kuwata-Gonokami, Phys. Rev. Lett. **76**, 2045 (1996).

[6] H. Saito and M. Ueda, Phys. Rev. Lett. **79**, 3869 (1997).

[7] H. Saito and M. Ueda, Phys. Rev. A **59**, 3959 (1999).

[8] Y. Yamamoto, F. Tassone, and H. Cao, *Semiconductor Cavity Quantum Electrodynamics,* Springer Tracts in Modern Physics Vol. 169 (Springer, Berlin, 2000).

[9] T.H. Oosterkamp, T. Fujisawa, W.G. van der Wiel, K. Ishibashi, R.V. Hijman, S. Tarucha, and L.P. Kouwenhoven, Nature (London) **395**, 873 (1998).

[10] T.H. Stoof and Yu.V. Nazarov, Phys. Rev. B **53**, 1050 (1996).

[11] R.H. Blick, D. Pfannkuche, R.J. Haug, K.v. Klitzing, and K. Eberl, Phys. Rev. Lett. **80**, 4032 (1998).

[12] R.H. Blick, D.W. van der Weide, R.J. Haug, and K. Eberl, Phys. Rev. Lett. **81**, 689 (1998).

[13] S. Tarucha, T. Fujisawa, K. Ono, D.G. Austin, T.H. Oosterkamp, and W.G. van der Wiel, Microelectron. Eng. **47**, 101 (1999).

[14] T. Fujisawa, T.H. Oosterkamp, W.G. van der Wiel, B.W. Broer, R. Aguado, S. Tarucha, and L.P. Kouwenhoven, Science **282**, 932 (1998).

[15] H. Qin, F. Simmel, R.H. Blick, J.P. Kotthaus, W. Wegscheider, and M. Bichler, Phys. Rev. B **63**, 035320 (2001).

[16] T. Brandes and B. Kramer, Phys. Rev. Lett. **83**, 3021 (1999).

[17] T. Fujisawa, D.G. Austing, Y. Tokura, Y. Hirayama, and S. Tarucha, Nature (London) **419**, 278 (2002).

[18] S. Debald, T. Brandes, and B. Kramer, Phys. Rev. B **66**, 041301(R) (2002).

[19] I. Wilson-Rae and A. Imamoglu, Phys. Rev. B **65**, 235311 (2002).

[20] E. M. Höhberger, J. Kirschbaum, R. H. Blick, T. Brandes, W. Wegscheider, M. Bichler, and J. P. Kotthaus (unpublished).

[21] H. Park, J. Park, A.K.L. Lim, E.H. Anderson, A.P. Alivisatos, and P.L. McEuen, Nature (London) **407**, 57 (2000).

[22] C. Joachim, J.K. Gimzewski, and A. Aviram, Nature (London) **408**, 541 (2000).

[23] Reichert, R. Ochs, D. Beckmann, H.B. Weber, M. Mayor, and H.v. Löhneysen, Phys. Rev. Lett. **88**, 176804 (2002).

[24] D. Boese and H. Schoeller, Europhys. Lett. **54**, 668 (2001).

[25] A.O. Gogolin and A. Komnik, cond-mat/0207513 (unpublished).

[26] A.N. Cleland and M.L. Roukes, Nature (London) **392**, 160 (1998).

[27] R.H. Blick, F.G. Monzon, W. Wegscheider, M. Bichler, F. Stern, and M.L. Roukes, Phys. Rev. B **62**, 17 103 (2000).

[28] N.F. Schwabe, A.N. Cleland, M.C. Cross, and M.I. Roukes, Phys. Rev. B **52**, 12 911 (1995).

[29] R.H. Blick, M.L. Roukes, W. Wegscheider, and M. Bichler, Physica B **249**, 784 (1998).

[30] A.D. Armour and A. MacKinnon, Phys. Rev. B **66**, 035333 (2002).

[31] L.Y. Gorelik, A. Isacsson, M.V. Voinova, B. Kasemo, R.I. Shek-

hter, and M. Jonson, Phys. Rev. Lett. **80**, 4526 (1998).

[32] C. Weiss and W. Zwerger, Europhys. Lett. **47**, 97 (1999).

[33] A. Erbe, C. Weiss, W. Zwerger, and R.H. Blick, Phys. Rev. Lett. **87**, 096106 (2001).

[34] N. Bannov, V. Mitin, and M. Stroscio, Phys. Status Solidi B **183**, 131 (1994).

[35] N. Bannov, V. Aristov, V. Mitin, and M.A. Stroscio, Phys. Rev. B **51**, 9930 (1995).

[36] N. Nishiguchi, Y. Ando, and M.N. Wybourne, J. Phys.: Condens. Matter **9**, 5751 (1997).

[37] M.P. Blencowe, Phys. Rev. B **59**, 4992 (1999).

[38] T.D. Kraus and F.W. Wise, Phys. Rev. Lett. **25**, 5102 (1998).

[39] X. Hu and F. Nori, Phys. Rev. Lett. **79**, 4605 (1997).

[40] M.P. Blencowe and M.N. Wybourne, Physica B **280**, 555 (2000).

[41] U. Hartmann and F.K. Wilhelm, Phys. Status Solidi B **233**, 385 (2002); U. Hartmann and F. K. Wilhelm, cond-mat/0212063 (unpublished).

[42] S.A. Gurvitz and Ya.S. Prager, Phys. Rev. B **53**, 15 932 (1996).

[43] S.A. Gurvitz, Phys. Rev. B **57**, 6602 (1998).

[44] D.F. Walls and G.J. Milburn, *Quantum Optics* (Springer, Berlin, 1994).

[45] T. Brandes and T. Vorrath, in *Recent Progress in Many Body Physics, Advances in Quantum Many Body Theory,* edited by R. Bishop, T. Brandes, K. Gernoth, N. Walet, and Y. Xian (World Scientific, Singapore, 2001).

[46] G. Doetsch, *Anleitung zum praktischen Gebrauch der Laplace-Transformation und der Z-Transformation* (Oldenbourg, München, 1989).

[47] T. Brandes and T. Vorrath, Phys. Rev. B **66**, 075341 (2002).

[48] R. Aguado and L. Kouwenhoven, Phys. Rev. Lett. **84**, 1986 (2000).

[49] K.E. Cahill and R.J. Glauber, Phys. Rev. **177**, 1882 (1969).

[50] S. Chountasis and A. Vourdas, Phys. Rev. A **58**, 848 (1998).

[51] I.S. Gradshteyn and I.M. Ryzhik, *Table of Integrals, Series, and Products,* 5 ed. (Academic, New York, 1994).